Ultrafast lasing due to electron–hole plasma in ZnO nano-multipods

2009 J. Phys.: Condens. Matter 21 064211

(http://iopscience.iop.org/0953-8984/21/6/064211)

J. Phys.: Condens. Matter **21** (2009) 064211 (5pp) doi:10.1088/0953-8984/21/6/064211

Ultrafast lasing due to electron–hole plasma in ZnO nano-multipods

S Mitsubori[1], I Katayama[2], S H Lee[3], T Yao[3] and J Takeda[1]

[1] Department of Physics, Yokohama National University, Yokohama 240-8501, Japan
[2] Interdisciplinary Research Center, Yokohama National University, Yokohama 240-8501, Japan
[3] Center for Interdisciplinary Research, Tohoku University, Sendai 980-8578, Japan

E-mail: jun@ynu.ac.jp (J Takeda)

Received 30 June 2008, in final form 12 August 2008
Published 20 January 2009
Online at stacks.iop.org/JPhysCM/21/064211

Abstract

Dynamics of stimulated emission and ultrafast lasing in ZnO nano-multipods has been investigated with a femtosecond optical Kerr shutter technique. Under band-to-band excitation with high density, stimulated emission is observed around 395–400 nm with a mode-like structure. The stimulated emission emerges with an onset time of ∼2 ps and then the intensity gradually decreases with time having a blue-shift and a spectral narrowing. The characteristics of the blue-shift and spectral narrowing suggest that not only recovery of bandgap renormalization but also conversion from an electron–hole plasma (EHP) state to high density excitonic state takes place as the carrier density decreases due to recombination of electrons with holes. The mode-like structure observed strongly indicates that a high quality resonant cavity is formed between the two facets toward the leg length direction of individual nano-multipod. These results show that the ultrafast lasing observed around 395–400 nm in ZnO nano-multipods comes from population inversion in the EHP regime. We also found that the initial carrier distribution of the EHP regime in nano-multipods is much wider than that in ZnO thin films, implying that the carrier diffusion might be suppressed by their nano-size structure.

1. Introduction

Because of the large bandgap energy (3.37 eV) and exciton binding energy (60 meV), ZnO-based materials represent promising candidates for ultraviolet (UV) optoelectronic devices such as UV lasers and light emitting diodes. Therefore the room temperature UV lasing for ZnO thin films as well as that for ZnO nanostructures has been extensively studied [1–6]. The lasing mechanisms are mainly classified into two categories: random lasing [1–3] and lasing from a resonator formed between the two facets of the nanostructures [4–6]. Most of the experimental studies in ZnO-based materials have been performed in steady-state measurements, while time-resolved studies to reveal the lasing dynamics have been very scarce. Therefore, time-resolved photoluminescence measurements with femtosecond time resolution are highly desired, which enable us to directly observe the ultrafast dynamics of the stimulated emission and its lasing properties.

In ZnO thin films, not only the stimulated emission due to the exciton–exciton scattering process (P emission) but also that due to the electron–hole plasma (EHP emission) was investigated with the femtosecond optical Kerr gate (OKG) technique [7–10]. At low excitation densities below the critical Mott transition density, the P emission, in which one of the two excitons scatters into a continuum state ($n = \infty$) and the other recombines radiatively, is observed around ∼390 nm (∼3.18 eV). The peak wavelength of the P emission shows a slight red-shift with time, and then stays at ∼390 nm without any spectral shift. The full width at half maximum (FWHM) of the P emission decreases with time and is close to ∼30 meV [7, 8]. These experimental results can be explained by taking account of both the initial energy distribution of the excitons formed by excitation laser pulses and cooling of the excitons due to acoustic phonons in the bottleneck region [7, 8]. At high excitation densities above the critical Mott transition density, on the other hand, the EHP emission is observed around ∼400 nm (∼3.1 eV) whose peak wavelength and FWHM depend on the excitation density [9, 10]. After buildup of the EHP emission in the early stage, the EHP emission band subsequently shows a

blue-shift and a decrease of the FWHM with time. The peak wavelength and FWHM of the EHP emission band after a long delay time are close to 390 nm and 30 meV, respectively; these values are almost the same as those of the P emission band observed in steady-state measurements [11]. These results strongly suggest that recovery of bandgap renormalization accompanied by conversion from the EHP state to high density excitonic state takes place as the carrier density decreases due to recombination of electrons with holes [9, 10].

Recently, lasing due to the exciton–exciton scattering process as well as that due to EHP has also been reported in a variety of novel ZnO nanostructures [4, 12]. In these studies, stimulated emission having mode-like sharp peaks is observed at 385–390 nm and is attributed to lasing due to the EHP regime judging from the high excitation density. However, as we mentioned above, in ZnO thin films, the photoluminescence due to the exciton–exciton scattering process is observed at the wavelength of 390 nm, while that due to the EHP regime is located around the longer wavelength region of ∼400 nm. Therefore the stimulated emission and lasing they observed lie at the wavelength region where the P emission should be. Also, the observed stimulated emission in ZnO nanostructures does not show a clear blue-shift and spectral narrowing with time, which is one of the important characteristics for the dynamics of the EHP emission.

To elucidate the stimulated emission and its lasing mechanism due to the EHP regime in ZnO nanostructures, in this paper, we investigate the time-resolved photoluminescence under band-to-band excitation with different excitation densities using the femtosecond OKG technique.

2. Experimental details

ZnO nano-multipods were grown on a Si substrate by a chemical vapor transport and condensation method using carbothermal reduction of ZnO powders [13]. The morphology of the samples was examined by scanning electron microscopy (SEM). A typical SEM image of ZnO nano-multipods is shown in figure 1. The typical leg length and diameter of ZnO nano-multipods are a few/several tens micron and a few hundreds nanometer, respectively.

Time-resolved luminescence spectra were measured at room temperature with the OKG technique, and were analyzed by a single monochromator combined with a charge coupled device cooled by liquid nitrogen [14, 15]. The third harmonic (267 nm, 4.65 eV) and fundamental laser pulses (800 nm, 1.55 eV) from a Ti:sapphire regenerative amplifier laser system with a 100 fs pulse duration and a repetition rate of 1 kHz were used as the excitation and gating pulses, respectively. The excitation fluence was varied from 2.2 to 13 mJ cm^{-2}. The spot size of the excitation at the sample was about 200 × 200 μm^2, which typically contains several nano-multipods (see figure 1). We used either CS_2 solution or a quartz plate with 1mm thickness as a Kerr medium. The Kerr medium was placed between two crossed polarizers. Time-integrated photoluminescence was measured with the same alignment as the time-resolved measurements, except that the two polarizers were set to a parallel configuration and the gating pulses were blocked. The overall time resolution of our apparatus is 1.2 ps for CS_2 while it is 400 fs for a quartz plate. The detailed experimental setup is almost the same as that reported in [14].

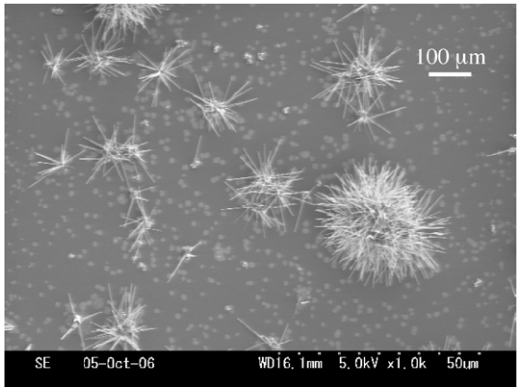

Figure 1. Typical SEM image of ZnO nano-multipods.

3. Results and discussion

Figure 2 shows two-dimensional time- and wavelength-resolved photoluminescence spectra in ZnO nano-multipods with different excitation fluences and sample positions, (a) 2.2 mJ cm^{-2}, (b) 5.1 mJ cm^{-2}, (c) 8.9 mJ cm^{-2} at a sample position A, and (d) 13 mJ cm^{-2} at a sample position B. The sample position A contains ZnO nano-multipods with typical leg length of 40–50 μm, while the sample position B includes those with the shorter leg length of ∼30 μm. The time-integrated luminescence spectra are also shown at the bottom of the figures. Under the low excitation fluences ((a) and (b)), the stimulated emission having mode-like sharp peaks is observed around 385–390 nm. Judging from the low excitation fluences and the peak wavelength of the emission band, the emission is considered to come from an inelastic scattering process of excitons (P emission). The P emission emerges with an onset time of 4 ps, and then the intensity decreases with time having a very small red-shift (see dotted curve in (b)). Under the high excitation fluences ((c) and (d)), on the other hand, the stimulated emission with mode-like structures, whose FWHM in the early stage is much broader than that under the low excitation fluences, is observed around 390–400 nm. This wavelength region is expected to have a stimulated emission of luminescence and lasing due to the EHP regime. The emission emerges with an onset time of 2–3 ps, and then shows an apparent blue-shift to shorter wavelength with time. Finally the emission seems to transform into the P emission (see the dotted curve in (d)). Judging from the high excitation fluences, the peak wavelength of the emission band, and the characteristics of the spectral shift and FWHM, the stimulated emission observed around 390–400 nm comes from the EHP regime.

The stimulated emissions both in the P and EHP regimes have an onset time of a few ps. Under band-to-band excitations, photoexcited electron–hole pairs have huge excess energy, and thus the carrier- (or exciton-) LO-phonon scattering process should effectively take place at an early

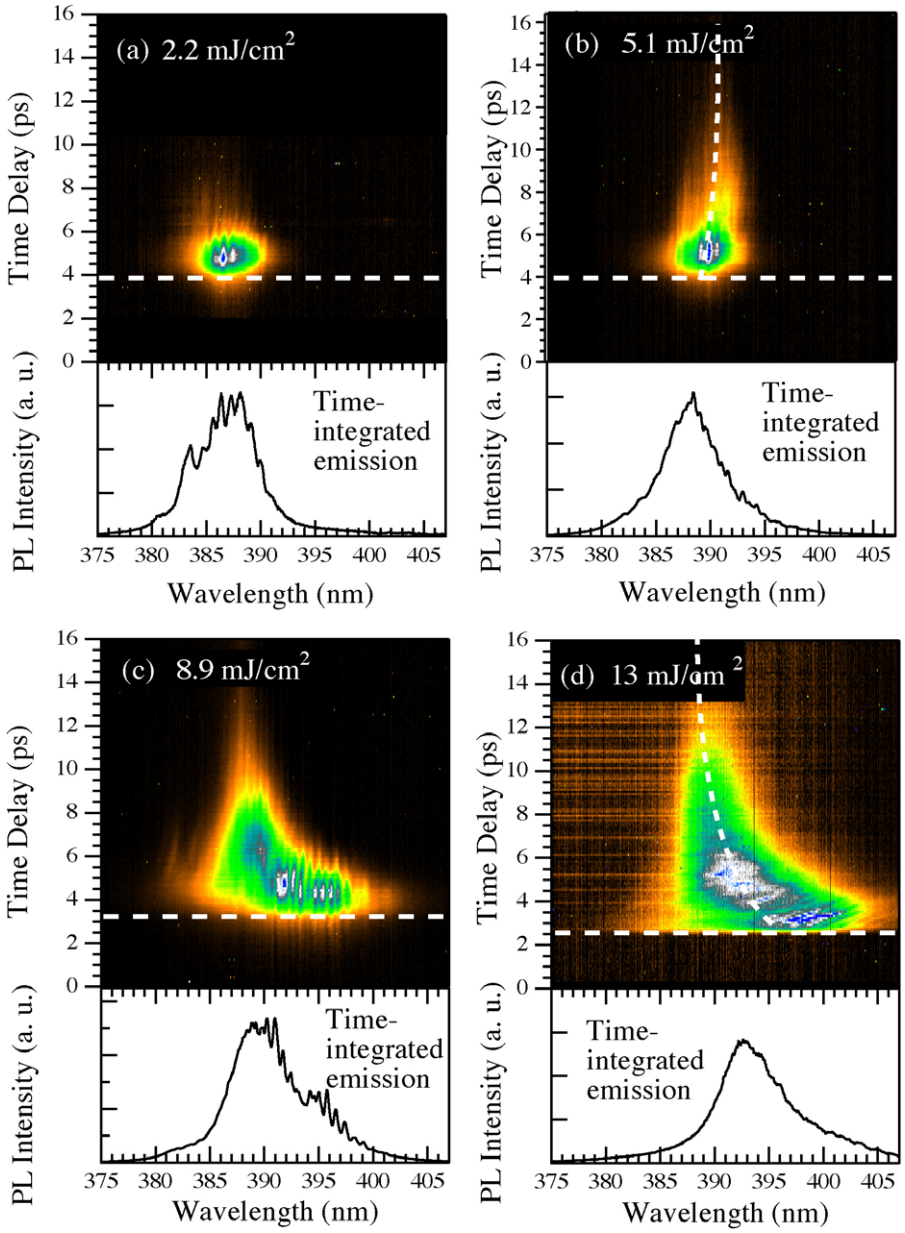

Figure 2. Two-dimensional time- and wavelength-resolved photoluminescence in ZnO nano-multipods with different excitation fluences. The time-integrated photoluminescence spectrum is also shown at the bottom of each figure. The onset time of the photoluminescence is shown by a dotted line in each figure.

(This figure is in colour only in the electronic version)

stage in comparison with radiative decay and carrier–carrier (exciton–exciton) scattering processes. After emitting multiple LO-phonons toward the band bottom, the stimulated emission subsequently appears with an onset time of a few ps because of the radiative decay process being dominant. The same behavior was also observed in ZnO thin films [7–10].

The most striking feature of the emission bands in ZnO nano-multipods is sharp mode-like structures observed just after the onset time of the emission bands. This indicates that ultrafast lasing takes place both in the P and EHP regimes. To reveal the sharp mode-like structures and the spectral shift of the emission bands in the EHP regime, time-resolved photoluminescence spectra in the EHP regime with different time delays are shown in figure 3. The sharp mode-like structure due to the lasing is located around 395 nm under the excitation fluence of 8.9 mJ cm^{-2}, while it lies at ∼400 nm under the excitation fluence of 13 mJ cm^{-2}. Since the observed wavelength region is lower than the P emission wavelength, the lasing observed at 395–400 nm must come from population inversion in the EHP regime. As far as we know, this is the first clear observation of ultrafast lasing in the EHP regime. Next, we will discuss the resonant cavity in ZnO nano-multipods. Assuming a Fabry–Perot laser cavity, the cavity length L is simply expressed as $L = \lambda_m\lambda_{m+1}/2n(\lambda_m - \lambda_{m+1})$, where $n = 2.45$ is the refractive index of ZnO [16]. From the mode distances observed, the cavity length in the sample position A

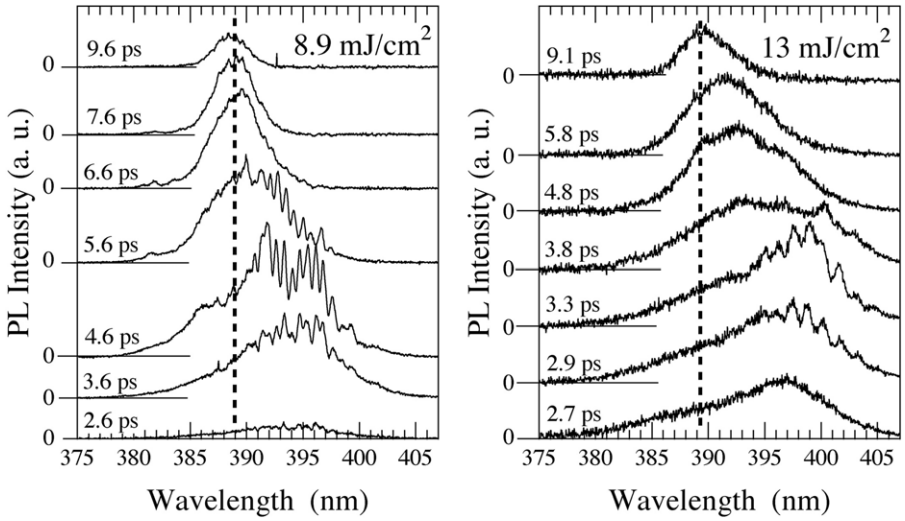

Figure 3. Time-resolved photoluminescence spectra with different time delays from ZnO nano-multipods in the EHP regime.

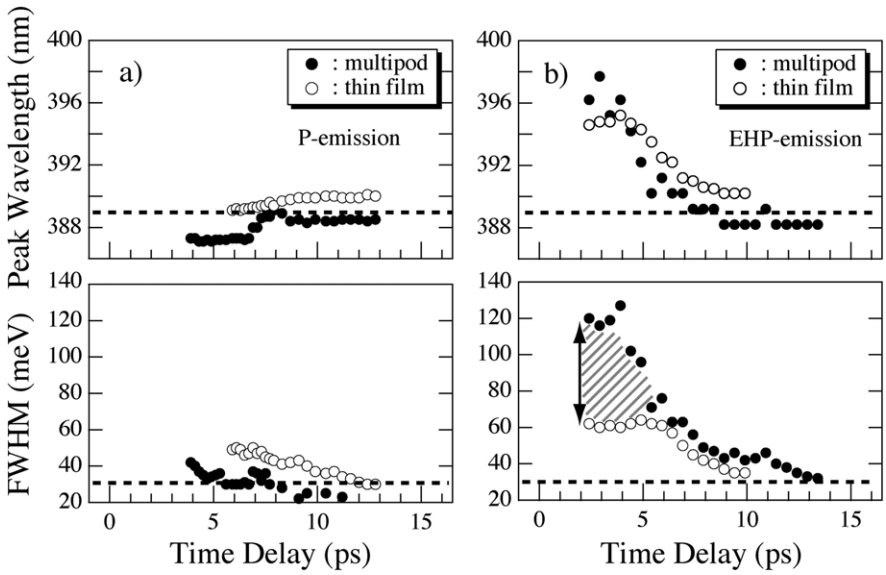

Figure 4. Peak wavelength and FWHM of the photoluminescence due to the P (a) and EHP (b) regimes in ZnO nano-multipods (closed circles) and thin films (open circles) as a function of time delay. The peak wavelength and the FWHM of the P emission estimated from the steady-state measurement [11] is shown by dotted lines.

is estimated to be 41 ± 9 μm, while that in the sample position B is 27 ± 6 μm. These values are in good agreement with the typical leg lengths of each sample position. Thus we conclude that a high resonant cavity is formed between the two facets toward the leg length direction of ZnO nano-multipods.

Finally, we compare the ultrafast dynamics of the stimulated emissions in ZnO nano-multipods with that in ZnO thin films previously reported [7–10]. Figure 4 shows the peak wavelength and FWHM of the stimulated emission bands due to the P (a) and EHP (b) regimes in ZnO nano-multipods (closed circles) and thin films (open circles) as a function of time delay. The peak wavelength and the FWHM of the P emission estimated from the steady-state measurement are also shown by dotted lines. In the P regime, the temporal behavior of the peak wavelength and FWHM of the stimulated emission are essentially the same between ZnO nano-multipods and ZnO thin films, although the onset time is slightly different. In the EHP regime, values of the peak wavelength and the FWHM of the EHP emission decrease with time and are close to those of the P emission observed in steady-state measurements after ~10 ps (see dotted lines in figure 4(b)). Therefore the carrier lifetime in the EHP regime is roughly estimated to be ~10 ps both in ZnO nano-multipods and ZnO thin films. On the other hand, the FWHM of the stimulated emission band at an early stage is quite different between ZnO nano-multipods and ZnO thin films (see hatched area in figure 4). The FWHM of the emission band in ZnO nano-multipods is about twice as wide as that in ZnO thin films at the time delay of 2 ps as shown by an arrow. The broad FWHM of the emission band generally implies that the photoexcited electron–hole system is hot, that is, the effective temperature of the system is relatively high. Here, we qualitatively speculate the reason why the

photoexcited electron–hole system of the EHP regime in ZnO nano-multipods is thermally hot in comparison with that in ZnO thin films, by taking account of the carrier diffusion effect. The carrier diffusion coefficient D in the EHP regime was estimated to be 10.8 $cm^2\ s^{-1}$ by femtosecond transient grating spectroscopy combined with a phase mask [17]. Therefore the diffusion length $L_D = \sqrt{D\tau}$ is calculated to be ∼100 nm when we use $D = 10.8\ cm^2\ s^{-1}$ and the carrier lifetime $\tau \approx 10$ ps. The estimated diffusion length L_D is comparable with the typical leg diameter of a few hundreds nanometer. Since the carrier diffusion in the radial direction is limited by the leg structure having nano-size diameter, cooling of the photoexcited carriers might be suppressed, leading to the broad emission band in the early stages.

In conclusion, dynamics of the stimulated emission and ultrafast lasing in ZnO nano-multipods were investigated under band-to-band excitations using OKG photoluminescence spectroscopy in the femtosecond time regime. Under high excitation fluences, a clear transition from the lasing due to the EHP regime to the stimulated emission due to the P regime is observed. The lasing due to the EHP regime comes from a high resonant cavity formed between the two facets of ZnO nano-multipods. By comparing the time-evolved experimental results in ZnO nano-multipods with those in ZnO thin films, we found that photoexcited electron–hole pairs in the EHP regime initially show a broad distribution in ZnO nano-multipods, which might come from suppression of the carrier diffusion by the nano-size structure of each ZnO nano-multipod.

Acknowledgments

This work is supported in part by the Grant-in-Aids for Scientific Research (A) from The Japan Society for the Promotion of Science (JSPS), and for Scientific Research on Priority Areas 'Development of New Quantum Simulator and Quantum Design' from The Ministry of Education, Culture, Sports, Science and Technology (MEXT).

References

[1] Cao H *et al* 1998 *Appl. Phys. Lett.* **73** 3656
[2] Yu S F *et al* 2004 *Appl. Phys. Lett.* **84** 3241
[3] Hsu H C *et al* 2005 *J. Appl. Phys.* **97** 064315
[4] Leung Y H *et al* 2005 *Nanotechnology* **16** 579
[5] Johnson J C *et al* 2004 *Nano Lett.* **4** 197
[6] Huang M H *et al* 2001 *Science* **292** 1897
[7] Toshine Y, Takeda J, Ko H J and Yao T 2004 *Phys. Status Solidi* c **1** 839
[8] Takeda J *et al* 2006 *Japan. J. Appl. Phys.* **45** 6961
[9] Takeda J, Kurita S, Chen Y F and Yao T 2001 *Int. J. Mod. Phys.* B **15** 3669
[10] Takeda J, Jinnouchi H, Kurita S, Chen Y F and Yao T 2002 *Phys. Status Solidi* b **229** 877
[11] Bagnall D M, Chen Y F, Zhu Z, Yao T, Shen M Y and Goto T 1998 *Appl. Phys. Lett.* **73** 1038
[12] Djurisic A B 2005 *J. Phys. Chem.* B **109** 19228
[13] Lee S H *et al* 2006 *J. Nanosci. Nanotechnology* **6** 3351
[14] Takeda J *et al* 2000 *Phys. Rev.* B **62** 10083
[15] Takeda J *et al* 2000 *J. Lumin.* **87–89** 927
[16] Zou B *et al* 2006 *J. Phys. Chem.* B **110** 12865
[17] Takeda J *et al* 2004 *Phys. Status Solidi* c **1** 678